

A WAVELET-BASED BRIDGE WEIGH-IN-MOTION SYSTEM

B. Lechner¹, M. Lieschnegg¹, O. Mariani¹, M. Pircher², A. Fuchs¹

¹Virtual Vehicle Competence Center

Inffeldgasse 21a, 8010 Graz, Austria

²Advanced Bridge Engineering Systems

Bergmannngasse 7, 8010 Graz, Austria

Email: bernhard.lechner@v2c2.at

Abstract- Bridge Weigh-in-Motion systems can be used to estimate vehicle parameters such as velocity, axle loads, or the distance between axles without affecting the traffic. These parameters and the classification of vehicles are necessary to determine vehicle overload and hence may help to reduce risks for road users and road infrastructure and allow optimized planning of maintenance work.

The Bridge Weigh-in-Motion system developed is based on a crack displacement sensor with intelligent data processing algorithms: In a first step, the number of axles, the distance between axles, and the velocity of the vehicle is obtained from the crack displacement signal by means of wavelet decomposition. In a subsequent step, the axle loads are found by means of optimizing the weights for axle loads that the measured crack displacement signal can be approximated by a superposition of (shifted and extended/compressed) ‘Lines of Influence’. Intensive test runs have been performed to verify results of the Bridge Weigh-in-Motion system.

Index terms: Bridge Weigh-in-Motion System, Wavelet Decomposition, Axle Load, Distance between Axles, Velocity Determination

I. INTRODUCTION

Weigh-in-motion (WIM) systems are used to determine axle loads, the distance between axles, the total weight and the velocity of vehicles. These parameters are obtained while the car or truck is moving, which allows to inspect much more vehicles at the same time than with a static weighing method. Studies reveal that trucks are currently checked for overload only every 30 years, even if the truck is in daily use [1]. The number of accidents as well as the damage of road infrastructure caused by overloaded trucks is assumed to be significant. Therefore, WIM systems

are also used to obtain information on the degree of infrastructure damage [2] and behavior of larger numbers of vehicles. A further field of application is the calibration of bridge rating via Eurocode [3].

We basically distinguish between WIM systems that are mounted on the road surface and systems that are mounted underneath a bridge to provide a signal that allows classifying vehicles. The second type of WIM systems are also called 'Nothing on the road' (NOR) systems [4].

A common WIM system is based on wheel scales that are integrated into the road surface. These systems can be easily calibrated by means of static methods and allow to determine directly the axle load. Even though wheel scales provide reasonable accuracy for lower vehicle velocities, these systems are rarely employed nowadays since maintenance is costly and the traffic has to be interrupted during service actions.

Load sensors based on strip lines are more commonly used: Thin wires with a cross section of a few mm^2 to cm^2 are installed in the road surface. The pressure-, force-, and drag influence is measured while a vehicle passes the test section. An integrating method is required since only a small part of the tire affects the measurement section. Even though the accuracy for the strip line system is typically lower than for the wheel scales due to the integrating measurement method, installation is significantly easier.

For systems mounted underneath a bridge (also called Bridge-WIM systems or B-WIM systems), the elongation underneath the bridge is measured. The elongation is typically measured by means of strain gauges or inductive displacement sensors and B-WIM systems have the advantage that maintenance and calibration does not affect the traffic at all.

To determine the vehicle velocity, the distance between axles and the axle load, current B-WIM systems require multiple sensors per lane, causing extra costs for installation and maintenance and significantly higher energy consumption during operation. Operating a WIM system that requires only one single sensor that can be powered by a battery or a solar panel has hence multiple advantages.

In this work, a B-WIM system with one single displacement sensor and the wavelet-based signal processing approach to determine vehicle velocity, the distance between axles, and the axle load are presented. Measurement results for a real-life application at two bridges are provided.

II. MEASUREMENT SETUP

For the measurements on the Austrian road B64 between the cities of Weiz and Gleisdorf, linear variable differential transformer (LVDT) displacement sensors with a detection limit of 30 nm have been mounted underneath the Salmbach bridge and the Arndorfbach bridge. For both bridges, the changes in the widths of existing cracks due to traffic loading have been monitored by means of these displacement sensors.

The sensors were mounted on one side of a crack using bolted and glued connections with the deck. Figure 1 shows the measurement setup with the displacement sensor and the crack underneath the bridge. Most B-WIM systems are measuring the elastic bending of the bridge. However, measuring the crack width results in a significant increase of sensitivity as the crack width responds much more to traffic loading than elastic bending.

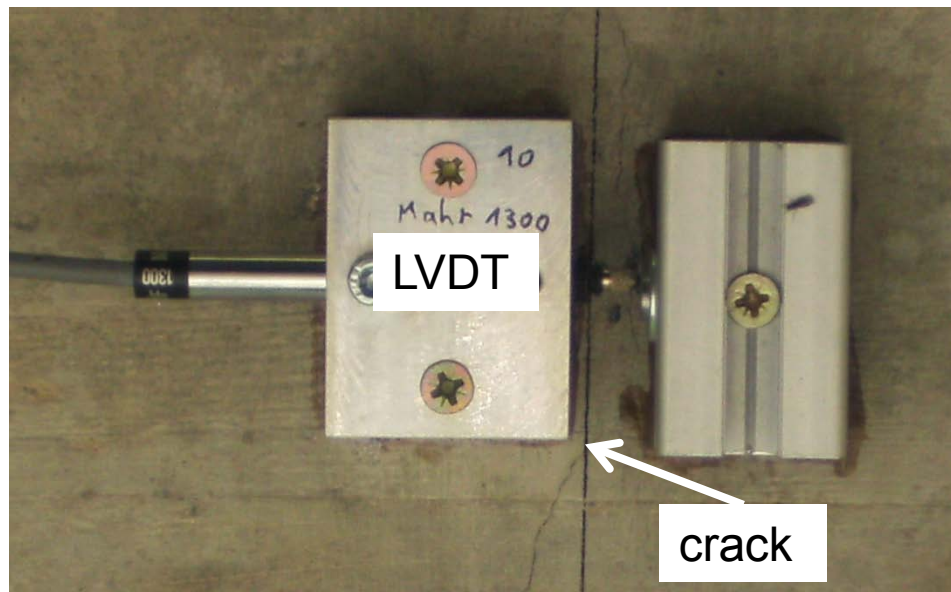


Figure 1: LVDT-sensor installed underneath the bridge and existing crack in the bridge structure

a. Infrastructure: the Salmbach bridge and the Arndorfbach bridge

Road B64 in the province of Styria, Austria, links an area with industrial and agricultural activity with the major highway network. Around 13,000 vehicles pass the Salmbach bridge on an average work day. A large proportion of these trucks serve the industrial fabrication yards along

this roads, and also deliver agricultural goods from and to farms in that particular area. Road B64 is also used by special transport vehicles, which move heavy industry products.

The Salmbach bridge (Figure 2a) was built in 1993 and is a slightly skew simply-supported slab bridge with a width of 13 m and a spanning of 7.5 m. Only some cracks in transversal direction could be observed on the underside of the deck slab. The Salmbach bridge is located close to a road junction and hence has three lanes with the middle lane assigned to turn off. The two lanes are hence rather far away from each other and hence have only little mutual impact. For the Salmbach bridge with its small span length, the variation of the crack width is just between $0.3 \mu\text{m}$ and $10 \mu\text{m}$ depending on the axle load. Due to the road junction nearby, accelerating and breaking vehicles have an impact on the accuracy of the measurement results.

The Arndorfbach bridge (Figure 2b) is a 3-span slab bridge with a span arrangement of $6.3+12.6+6.3$ m. There are elastomeric bearings at the abutments and hinged connections between piers and the deck. The bridge was built in 1967. Some cracks in the transversal direction could be observed on the underside in the middle of bridge. Also for the Arndorfbach bridge, the variation of the crack width is in a similar range as for the Salmbach bridge, but the dynamic effects are more significant for the middle segment of the bridge.



(a)



(b)

Figure 2: Bridges investigated in this work: (a) Salmbach bridge and (b) Arndorfbach bridge

III. MEASUREMENT PROCEDURE

The response of the bridges to vehicle load was measured by calibration runs with two heavy duty vehicles and a passenger car of known axle weights, axle spacing and velocity (see Table 1). During the calibration runs the bridges were closed for traffic. The bridges were permanently monitored from June 28, 2009 until October 20, 2009 with a sampling rate of 200 Hz. During the calibration runs the sampling rate was increased to 500 Hz. The velocity of the vehicles was measured using light barriers for reference purpose.

Table 1 Parameters of the calibration vehicles (parameters obtained by means of wheel scales)

Vehicle	Axle Load [kg]			Axle spacing [m]		
	Axle1	Axle 2	Axle 3	Axle 1-2	Axle 2-3	Total Length
PC	1240	980		3.030		3.030
HDV2 (2 Axles)	8090	11145		3.900		3.900
HDV3 (3 Axles)	8970	7672	8774	5.100	1.350	6.450

A passenger car was used to check the response of the bridge for small axle loads and to check the detection limit. The heavy duty reference vehicles with two axles (HDV2) served for the investigation of higher axle load and the HDV3 served for the detection of axles within an axle group.

The axle loads are measured using wheel scales of the type RW 8.2 from HKM and a measurement range of 0 to 8,000 kg. The accuracy of these wheel scales is ± 10 kg for a load under 5,000 kg and ± 15 kg for a load above 5,000 kg. However, for the correct measurement of axle loading the vehicle has to be carefully balanced. So, the accuracy of the wheel scales given above is not achieved in a real-world measurement. To check the accuracy the gross vehicle weight (GVW) was measured on a weighbridge. The deviation of the GVW measured with the two methods was up to 4%.

On September 9, 2009 for half an hour all passing vehicles were videotaped and the videotaping was synchronized to the measurement data. So a certain crack width signal can easily be assigned to a passing vehicle.

A data acquisition system USB 6212 of National Instruments was used. Data acquisition and data evaluation was done using LabView 2009.

All heavy duty vehicles are classified by their axle number and axle spacing [5] e.g. type 8 is a simple HDV with two axis (HDV2 of the calibration runs), type 9 is an HDV with two axes groups where the second axes group consists of two axes (HDV2 of the calibration runs), type 12 is a four-wheel HDV, type 97 has three axes groups where the third group consists of two axes, while the third axes group of type 98 consists of three axes. The latter one is the most frequent type of HDV. This classification is necessary to determine the ‘stress’ and furthermore the realistic ‘aging’ of the bridge for better planning of maintenance.

Although the Salmbach bridge and the Arndorfbach bridge are both rather small bridges, the sensor setup is that sensitive that even the influence of passenger cars could be observed reliably.

IV. ALGORITHMS AND MATHEMATICAL METHODS

The determination of the vehicle velocity, the number of axles, and the distance between axles is done in this work by means of wavelet decomposition of the displacement sensor signal. This method was first introduced by Chatterjee [6] and makes use of the mathematical similarity of Lines of Influence (LoI) and a wavelet. In a subsequent optimization step, the axles are assigned a certain weight by means of a least square algorithm that the displacement signal can be approximated using superposition of LoIs.

a. Wavelets

Wavelets are mathematical objects that can be found in several technical disciplines and applications such as data compression or image recognition. In this work we just give the necessary information about wavelets to explain the algorithms proposed. For a detailed description of wavelets we refer to [6] and [7].

A wavelet is defined as:

1. Starting from a mother wavelet Ψ , all wavelets $\Psi_{s,\tau}$ of the same family are generated by compression or expansion s and a time delay τ .

$$\Psi_{s,t}(t) = \frac{1}{\sqrt{|s|}} \Psi\left(\frac{t - \tau}{s}\right) \quad (1)$$

2. The wavelets generated from one mother wavelet define an orthonormal basic system, i.e. they are all orthonormal.

$$\int_{t=-\infty}^{t=\infty} \psi_{s,\tau}(t) \psi_{s',\tau'}^*(t) dt = \delta_s^{s'} \delta_\tau^{\tau'} \quad (2)$$

3. Each function $x(t)$ can be described by a linear combination of wavelets.

$$x(t) = \int W_\psi(s, \tau) \psi_{s,\tau}(t) d\tau ds \quad (3)$$

$W_\psi(s, \tau)$ are the wavelet coefficients of function $x(t)$. They are calculated via the scalar product:

$$W_\psi(s, \tau) = \int x(t) \psi_{s,\tau}^*(t) dt \quad (4)$$

Generally, the calculation of wavelet coefficients could be done directly using (4) for each wavelet, but more efficient algorithms (e.g. multiresolution analysis, [9]) are available that allow calculation of wavelet coefficients analogous to the Fast-Fourier-Transformation (FFT).

b Scale Factor

Wavelet coefficients depend on the scale factor s and time t . The scale factor in wavelet decomposition can be compared to the frequency in Fourier transformation. For a low scale factor, details in the signal can be obtained. Hence a low scale factor corresponds to a high frequency in FFT. For a high scale factor – analogous to low frequencies in FFT – only broad bands are obtained.

c Line of Influence

The LoI represents the expansion of the bridge at a given position (e.g. at the position of the sensor) for a punctiform load. The shape of the LoI only depends on the load (i.e. the amplitude of the signal is affected) and the velocity of the load passing the bridge (i.e. the time basis of the LoI is compressed or extended).

Starting from one “mother-LoI”, each additional LoI can be generated by means of compression, extension, amplification, and time delay. Hence, LoIs have a crucial similarity with the properties of wavelets. The LoIs can be determined by recording displacement data for a reference vehicle with known distance between axles and known axle load. A determination of the LoI by means of standard Finite Element Method approaches is also possible.

d. Determination of Vehicle Velocity

To describe the measured crack displacement signal as a superposition of LoIs, the velocity information must be available. The time Δt_1 , when a vehicle is on the bridge can be easily determined since the crack displacement varies significantly from the baseline. Using wavelet decomposition, the time difference Δt_2 between the first and the last axle is obtained. With the known spanning l_1 of the bridge, the velocity calculates to

$$v = \frac{l_1}{\Delta t_1 - \Delta t_2} \quad (5)$$

The length of the vehicle l_2 calculates to

$$l_2 = \frac{\Delta t_2}{v} \quad (6)$$

e. Optimization to Obtain Axle Loads

The crack displacement signal $x(t)$ caused by a vehicle with n axles can be approximated by linear superposition of the LoI of the n axles:

$$x(t) = \sum_{i=1}^n a_i L \left(\Theta - \Delta \tau_i t \right) + e \quad (7)$$

with a_i as the weight of the i^{th} axle. s_i is the distance between axles and $\Delta \tau_i$ the time delay of the i^{th} axle, determined by:

$$\tau_i = \frac{s_i}{v} \quad (8)$$

The term e denotes effects that cannot be described by the model (e.g. oscillation of the bridge caused by vehicles, braking and acceleration of vehicles, impact of the opposite lane, measurement errors, etc.)

The parameters $\Delta \tau_i$ and a_i have both been estimated by means of wavelet decomposition. Since the LoI is not a wavelet, the parameters can only be estimated with limited accuracy. Hence, the measured signal is approximated as a superposition of LoI by means of a least square fit.

For the experimental results it could be shown that the wavelet decomposition and the subsequent optimization can be performed on a standard personal computer in less than one second.

V. RESULTS

a. Results for Reference Vehicles

To quantify the quality of the developed B-WIM system, measurements with reference vehicles of known parameters have been performed. Figure 3 shows a trailer truck with three axle groups and five axles. The first two axle groups consist of one axle each and the third axle group of three axles. This type of trailer truck is the most common one and commonly referred as type 98.

Figure 4 shows the crack displacement signal caused by the passing HDV in Figure 3 at Salmbach bridge as a thick solid line. The wavelet coefficients for scale factors 1, 10, and 20 are also plotted in Figure 4. It can be seen that the choice of the scale factor has significant impact on the quality of the data for further processing.

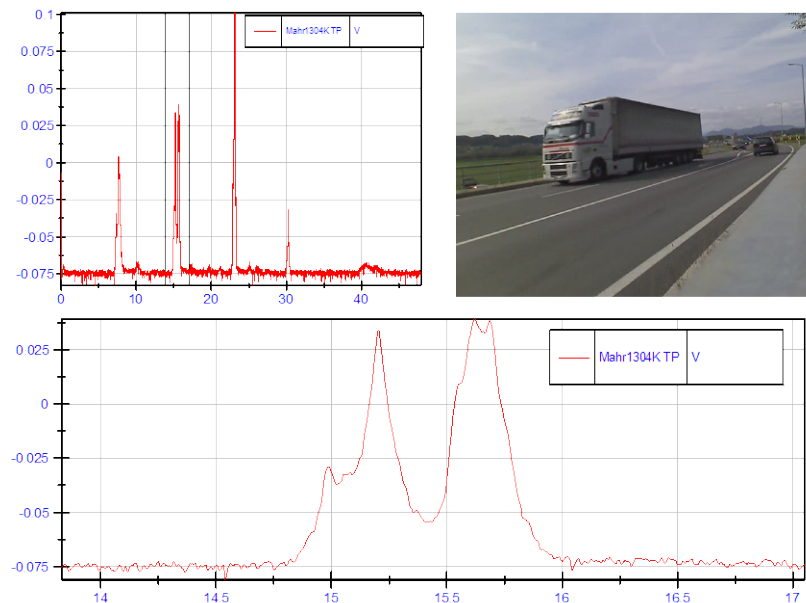


Figure 3: Passing HDV type 98 with 5 axles

In Figure 4, the wavelet decomposition with a scale factor of 1 results in noise (i.e. high frequency signal). For wavelet decomposition with a scale factor of 10, individual axles can be detected – the first axle is found at 0.49 s, the second axle at 0.7 s, and the group of axles (3, 4, and 5) is found between 1.0 s and 1.2 s. The resolution is decreasing with increasing scale factor, for a scale factor of 20 only groups of axles but no individual axles can be detected.

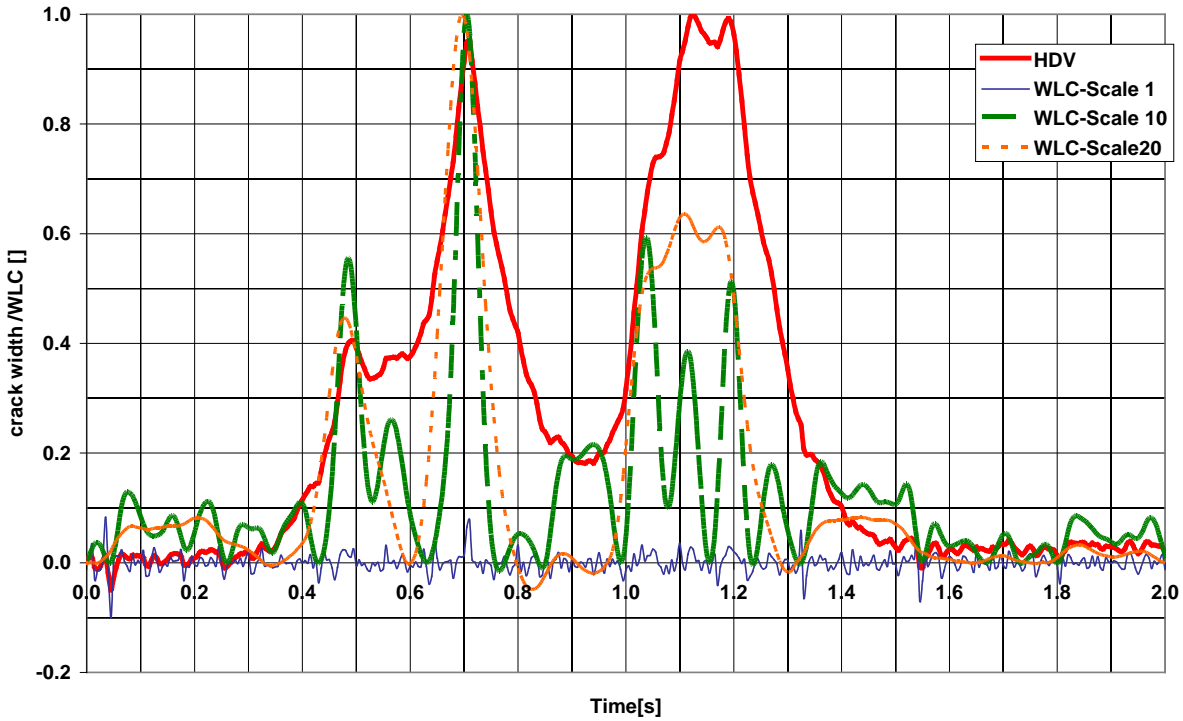


Figure 4: Signal of a HDV type 98 and wavelet decomposition with wavelet coefficients (WLC) at scale factor 1, scale factor 10 and scale factor 20.

The normalized LoI for the Salmbach bridge is shown in Figure 5. Due to the construction of the bridge, the crack at the Salmbach bridge is only expanded, while the crack at the second span at Arndorfbach bridge, which as a three-span bridge, is also contracted when a vehicle passes the first and the third span. Figure 5 also shows the mother wavelet *rbio2.2*, that has a similar shape as the LoI.

In a first step, we try to obtain results for vehicle velocity, axle number, distance between axles and an estimation of the axle loads from the sensor signal all by means of wavelet decomposition. In a subsequent step, axle loads are quantified by using optimization methods.

Figure 6 shows the passing of a 4 axle HDV (type 12). It can be seen that the third and fourth axle are close together.

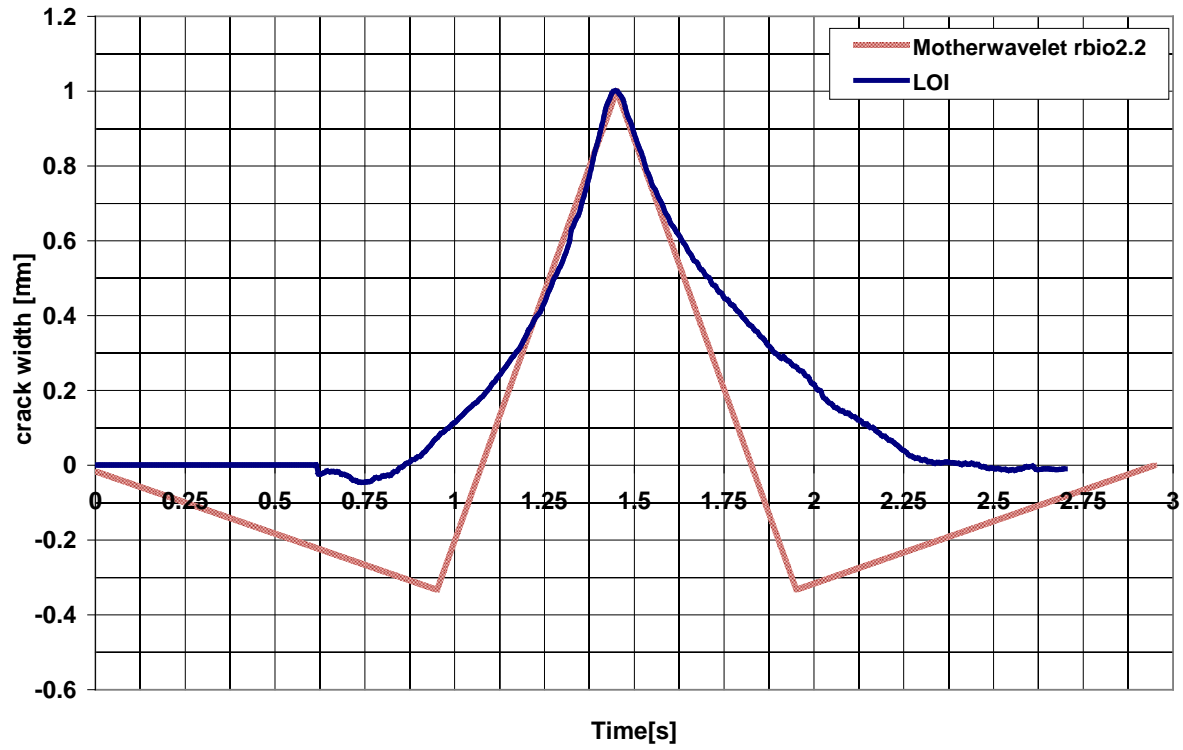


Figure 5: LoI for Salmbach bridge and mother wavelet rbio2.2

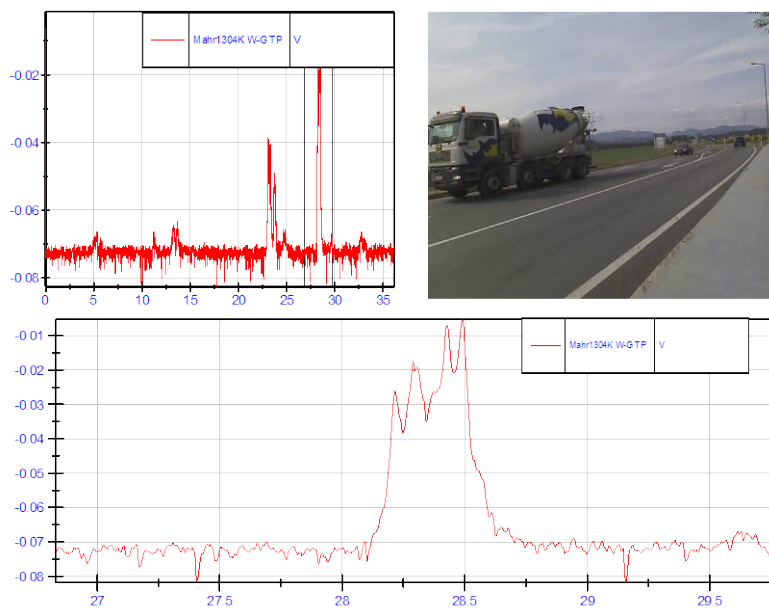


Figure 6 Passing of a 4 axle HDV (type 12)

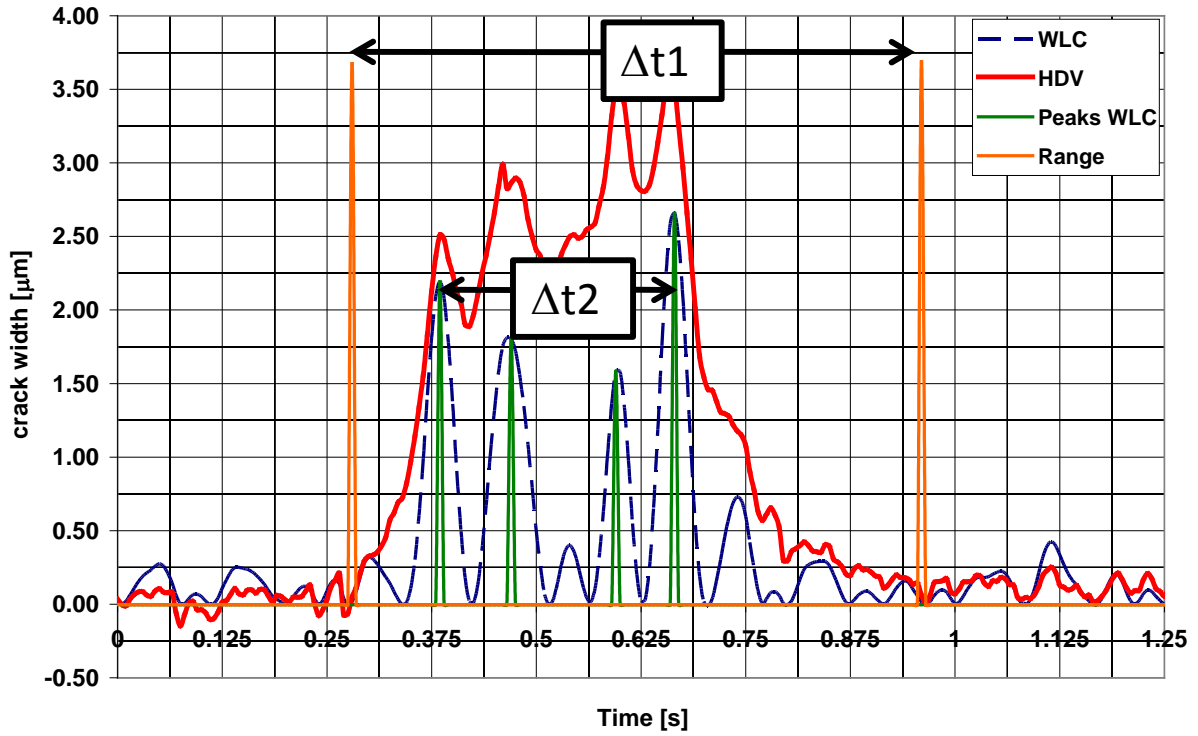


Figure 7: Crack displacement signal and wavelet coefficient (WLC) of the 4 axle truck shown in Figure 6

Figure 8 shows the crack displacement signal for the heavy duty vehicle in Figure 3. When the parameters obtained by the fast wavelet decomposition, we obtain the graph ‘Start’ in Figure 8. The parameters a_i in (3) can be determined by means of a least square fit.

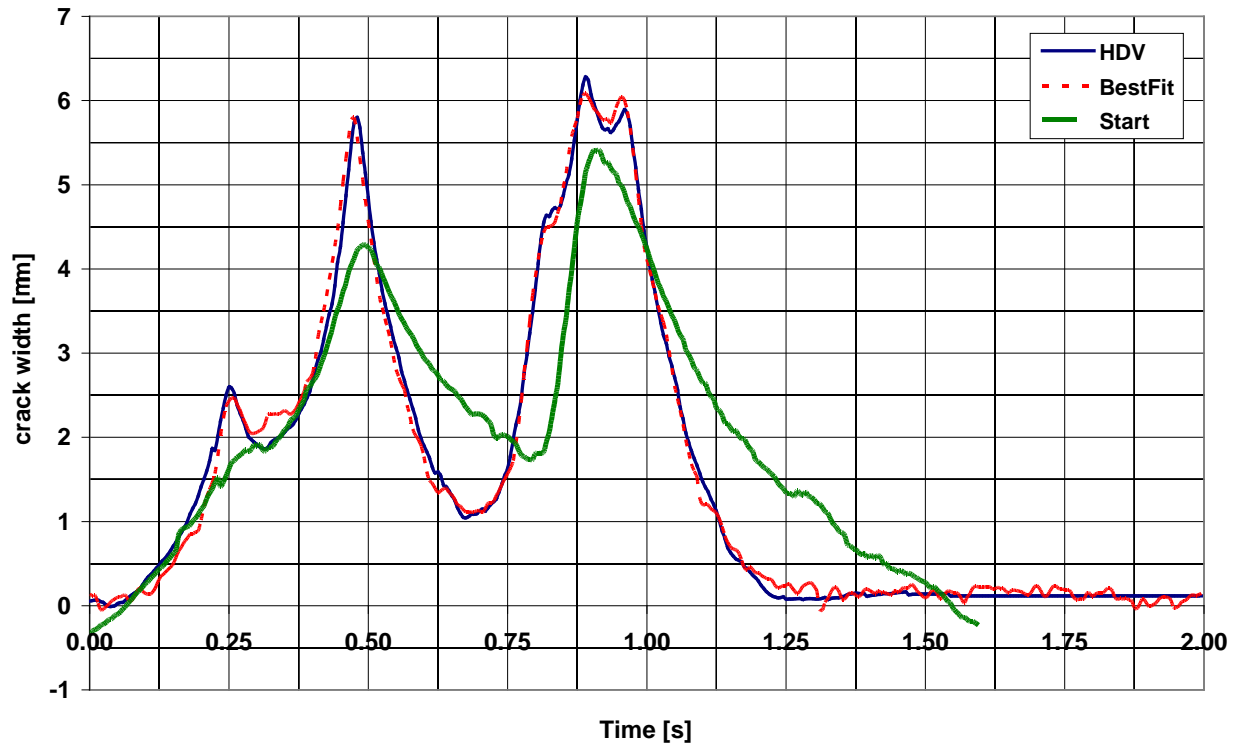


Figure 8 Optimization of the LoI

The B-WIM system built up can be tested by using reference vehicles with known axle loads and known distance between axles. Therefore, the road B64 has been closed for other vehicles and test with reference vehicles with axle loads from 900 kg to 8,000 kg and velocities from 2 km/h to 120 km/h have been performed. A camera has been installed to record the passing of the vehicles.

For the Arndorfbach bridge, four tests have been made per reference vehicle. The velocity of the vehicles has been recorded by means of two light barriers. A high speed test drive has been made with a passenger car with 118 km/h.

A (mother) LoI from the passing of the first axle of HDV2 at a velocity of 2.5 km/h has been generated. All other LoIs were generated using expansion and compression of the time basis.

Table 2 summarizes the results of the drives with the reference vehicles.

Table 2 Result of test runs with reference vehicles

Test run	Vehicle	Speed LB	Speed BWIM	Axle 1	Axle 2	Axle 3	GVW	Axle 1-2 spacing	Axle 2-3 spacing
		[km/h]	[km/h]	[to]	[to]	[to]	[to]	[m]	[m]
1	HDV3	3.90	3.8	8.38	8.54	8.4	25.32	5.176	6.58
2	HDV2	2.50	2.7	8.16	11.27		19.43	4.26	
3	PC	5.00	4.6	1.15	0.96		2.11	2.41	
4	HDV3	50.10	53	8.47	10.14	6.14	24.79	5.71	7.11
5	HDV2	46.00	55	7.96	10.88		18.84	4.67	
6	PC		49	1.18	0.95		2.13	3.14	
7	HDV3	75.20	79	8.41	8.16	8.69	25.26	5.9	7.6
8	HDV2	88.00	75	7.71	11.08		18.79	4.61	
9	PC		83	1.24	0.92		2.16	3.61	
10	HDV3	81.00	81	7.77	8.8	8.3	24.87	5.52	6.95
11	HDV2	70.00	80.6	7.29	10.99		18.28	4.51	
12	PC	118.00	152	1.16	1.03		2.19	4.18	

“Speed LB” in Table 2 is the speed measured using the light barriers, “Speed BWIM” was measured with the B-WIM system. There is a good agreement between these two systems for a velocity of up to 50 km/h and a somewhat larger deviation for higher velocities. This is due to the fact that a faster vehicle spends less time on the bridge and also causes higher dynamic effects and bridge oscillation.

Table 3 shows the deviations between measurement results between the wheel scales measurement of the reference vehicles and the B-WIM system. The total mass of the vehicles is determined well, the deviation is in most cases below 5%. Also the axle loads for the passenger car (PC) and HDV2 are determined reliably with an error in the range of $\pm 5\%$. While for the first axle of HDV3 the obtained value is good, the error for the second axle group is much higher and reaches 40% during two tests while the overall load of all axles is in good agreement. The signal of HDV3 is shown in Figure 3. The axles are indicated and the dynamic effects can be seen clearly. The third axle is somewhat lower than the second axle. Thus, the second axle is given too much weight by the B-WIM-system.

The deviation for the determination of the distance between axles is in the range of 15%. The only exception is the test with the PC with 118 km/h: Due to the weak measurement signal and the short measurement sequence, the velocity has been determined with significant uncertainty, which also affects the determination of the distance between the axles.

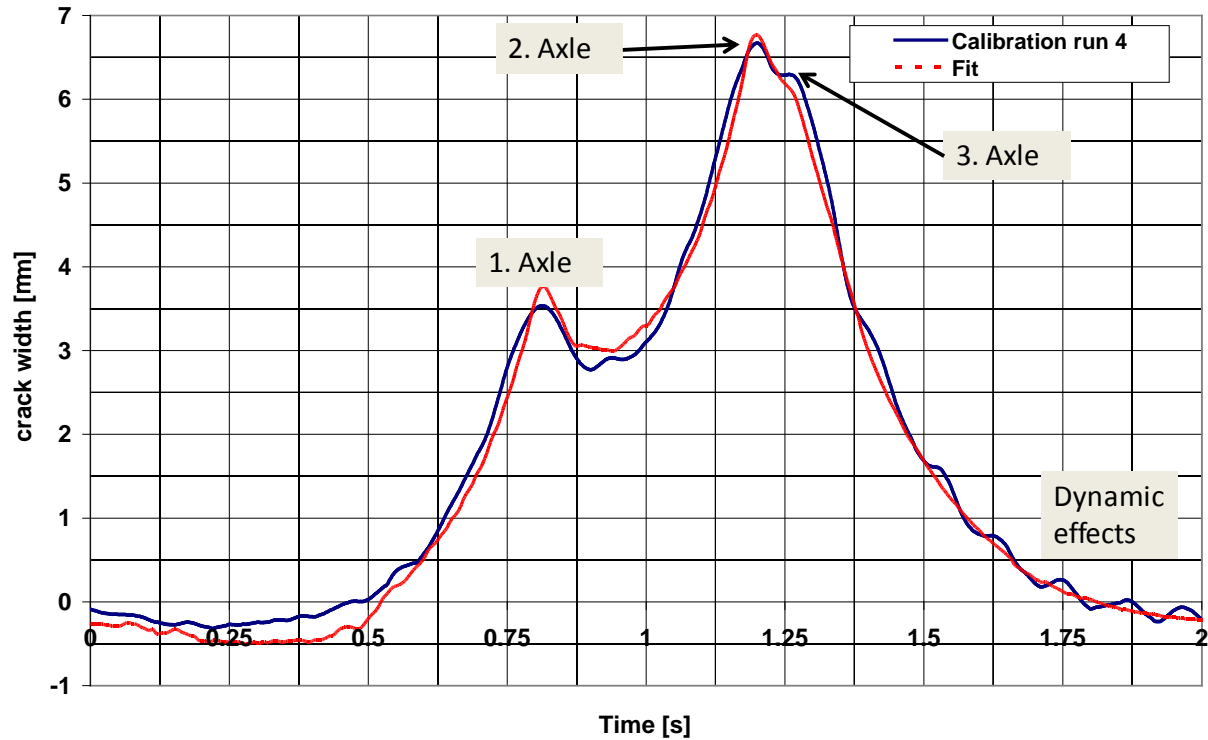


Figure 9: Crack displacement for test run number 4 and best fit

Table 3 Deviations between reference values and B-WIM results for test runs with reference vehicles

Calibration run	Vehicle	Axle 1	Axle 2	Axle 3	GVW	Axle 1-2 spacing	Axle 2-3 spacing
		[%]	[%]	[%]	[%]	[%]	[%]
1	HDV3	6.58	-11.31	4.26	0.38	-1.49	-2.02
2	HDV2	-0.87	-1.12		-1.01	-9.23	
3	PC	7.26	2.04		4.95	13.93	
4	HDV3	6.80	-42.86	37.66	2.46	-11.96	-10.23
5	HDV2	1.61	2.38		2.05	-19.74	
6	PC	4.84	3.06		4.05	-12.14	
7	HDV3	6.24	-6.36	0.96	0.61	-15.69	-17.83
8	HDV2	4.70	0.58		2.31	-18.21	
9	PC	0.00	6.12		2.70	-28.93	
10	HDV3	13.38	-14.70	5.40	2.15	-8.24	-7.75
11	HDV2	9.89	1.39		4.96	-15.64	
12	PC	6.45	-5.10		1.35	-49.29	

b. Results for Standard Traffic

After evaluating the performance of the B-WIM system with reference vehicles, measurements with standard traffic vehicles (i.e. parameters were not known a-priori) have been performed. 16 HDVs passing the Salmbach bridge were videotaped and synchronized to the measurement data. The results for the 16 vehicles are given in Table 4.

Due to the determined distance between axles, the axle loads, and the total weight, a classification according to [5] can be made automatically. The vehicle velocity is again also determined by means of light barrier (the measurement failed for HDV 3 and HDV 10 due to traffic on the opposite lane). With the videotape results the correctness of the automated vehicle classification can be verified.

Table 4: Results for 16 HDVs observed at Salmbach bridge

	Type	Speed LB	Speed B-WIM	Length vehicle	Axle Spacing				GVW	Type corr.
					1-2	2-3	3-4	4-5		
					[km/h]	[km/h]	[m]			
HDV 1	9	42.1	44	9.6	4.11	5.66	-	-	16.96	Yes
HDV 2	98	60.4	59.36	16.7	3.59	9.14	10.41	11.67	38.12	Yes
HDV 3	12	-	71.9	8.6	1.77	4.34	5.72		36.97	Yes
HDV 4	8	68	89		3.8				6.26	Yes
HDV 5	98	75	85	16.8	4.08	10.92	12.44	13.97	61.4	Yes
HDV 6	97	71	67	16.6	3.8	9.56	10.82		31.3	Yes
HDV 7	42	70.9	71.7	18.94	5.21	13.78			12.85	No
HDV 8	98	61	-	13.4						No
HDV 9	98	43.4	45.9	16.6	3.7	11.6			17.79	No
HDV 10	12	-	85.8		2.2	4.97	6.58		18.82	Yes
HDV 11	8	71.4	-	9.8	4.3				9.09	Yes
HDV 12	12	73.4	75.1	8.1	1.7	4.7	6.07		20.6	Yes
HDV 13	33	50	65.6	19.1	6.2	12.3	19.3		12.5	Yes
HDV 14	98	72.6	70.7	16.8	3.68	10.45	11.87		14.86	No
HDV 15	8	63.6	56.8	6.6	2.66				12.27	Yes
HDV 16	9	71.9	68.2	9.2	3.63	4.9			26.63	Yes

The determined vehicle velocities (light barrier and B-WIM system) are in good accordance for most vehicles. Velocity deviations could be found for HDV 13, a light HDV with unloaded trailer, where the B-WIM system could not detect reliably the time stamp when the trailer left the bridge.

In total, four HDVs could not be classified correctly. For all of these vehicles the number of axle groups was detected correctly, but triple axles have been identified as double axles (HDV 9 and HDV 14) or double axles have been identified as a single axle (HDV 7). HDV 8 was an unloaded rather light, tank truck that could not be identified due to the weak measurement signal.

The comparison of the vehicle length with the distance between axles for the HDVs shows, that the distance between axles can be determined by means of the B-WIM system with reasonable accuracy.

The major limitation for the accuracy of the B-WIM system developed seems to be vibrations of the bridge caused by (heavy) vehicles. Due to these dynamic effects the assumption in (3) that the crack displacement signal can be represented as a linear superposition of shifted LoIs is not fulfilled. Figure 10 shows the crack displacement signal of a tractor-trailer passing Arndorfbach bridge. Due to an uneven surface, the vehicle causes bridge oscillations that are in the same magnitude as the crack displacement due to the vehicle's weight. Using a band-stop filter to minimize the impact of oscillation was not successful since the signal is distorted. The most effective strategy seemed to be the use of higher scale values, although the resolution is reduced.

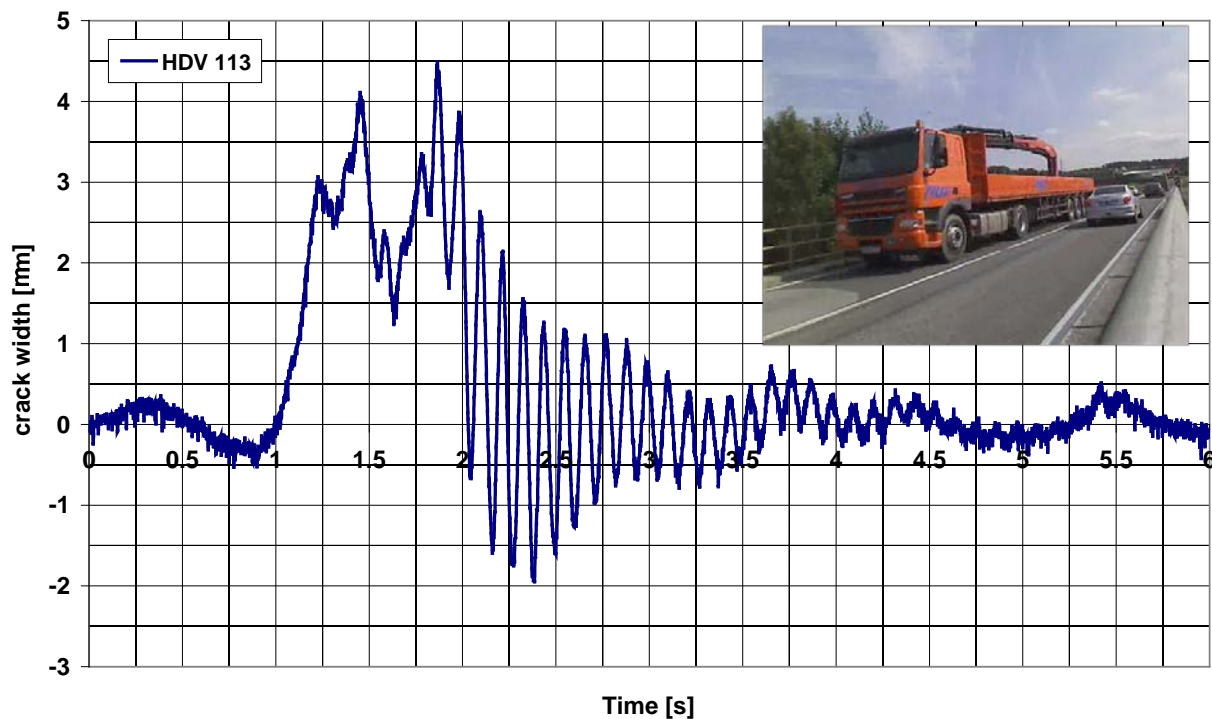


Figure 10 Dynamic effects of a passing HDV of type 98 at Arndorfbach bridge

VI. CONCLUSION

Overload of HDVs has a significant effect on safety and damage to infrastructure such as bridges. Currently, no practicable method for online determination of HDV overload is available. B-WIM systems can be used to estimate vehicle parameters such as velocity, axle loads, or the distance between axles without affecting the traffic.

A B-WIM system with one single sensor front-end (crack displacement sensor) and intelligent algorithms has been developed at the Virtual Vehicle Competence Center. In the course of a measurement campaign at the B64 road in Austria, two bridges have been equipped with this B-WIM system and data has been recorded for four months.

Data processing is done in a two-step strategy: The number of axles, the distance between axles, and the velocity of the vehicle is obtained from the crack displacement signal by means of wavelet decomposition. In a subsequent step, the axle loads are found by means of optimizing the weights for axle loads that the measured crack displacement signal can be approximated by a superposition of (shifted and extended/compressed) LoIs.

Test runs with vehicles of well-known parameters are used for verification of the B-WIM system. These tests show that the B-WIM system works reliable for most types of vehicles and provides results of good quality. Nevertheless, the oscillating behavior of bridges caused by heavy vehicles and uneven road surfaces on the bridge has a negative effect on the result quality. In certain cases, the determination of parameters and the classification of the vehicle failed.

The algorithms presented in this work have robust and fast performance. The developed B-WIM hardware and the algorithms have been successfully tested under real life conditions on two road bridges.

ACKNOWLEDGEMENT

The authors would like to acknowledge the financial support of the "COMET K2 - Competence Centres for Excellent Technologies Programme" of the Austrian Federal Ministry for Transport, Innovation and Technology (BMVIT), the Austrian Federal Ministry of Economy, Family and Youth (BMWFI), the Austrian Research Promotion Agency (FFG), the Province of Styria and the Styrian Business Promotion Agency (SFG).

We would furthermore like to express our thanks to our supporting industrial project partner Advanced Bridge Engineering Systems and to Graz University of Technology.

REFERENCES

- [1] B. Jacob B., V. Feypell-de la Beaumelle, "Improving truck safety: Potential of weigh-in-motion technology", IATSS Research 34, 9-15, 2010
- [2] M. Pircher, B. Lechner, O. Mariani, A. Kammersberger, „Schädigung einer schlaff bewehrten Betonbrücke durch Verkehrsbelastung“, Beton- und Stahlbetonbau, 104,154-163, 2009
- [3] DIN EN 1991-2, „Eurocode 1: Einwirkungen auf Tragwerke - Teil 2: Verkehrslasten auf Brücken“, Deutsche Fassung EN 1991-2:2003_
- [4] B. Jacob, S. Jehaes, "Weigh-in-Motion of Road Vehicles", Final Report of the COST323 2 Action, LCPC, Paris, 538 pp., 2004.
- [5] K.P. Glaeser et al., "Auswirkungen von neuen Fahrzeugkonzepten auf die Infrastruktur des Bundesfernnetzes", Schlussbericht, Bundesanstalt für Straßenwesen, Bergisch Gladbach 2006.
- [6] P. Chatterjee, E. O'Brien, Y. Li, A.González, "Wavelet domain analysis for identification of vehicle axles from bridge measurements", Computers & Structures, 84, 1792-1801., 2006.
- [7] I. Daubechies, "Ten lectures on wavelets", Society for Industrial Applied Mathematics. Philadelphia. Pennsylvania, 1992.
- [8] S. Mallat, "Multiresolution approximation and wavelets", Trans. Amer. Maths. Soc. 315, 69-88, 1989.
- [9] J. Trygg, S. Wold, "PLS regression on wavelet compressed NIR spectra", Chemometr. Intell. Lab. Syst. 42, 209-220, 1998